10.2478/v10048-012-0006-9

MEASUREMENT SCIENCE REVIEW, Volume 12, No. 1, 2012

Characterization of Microwave Antennas for Intracardiac Ablation Frequencies 915 and 2450 MHz

A. Rouane, D. Kourtiche

Laboratory of Electronic Instrumentation of Nancy; Lorraine University; BP 70239;
Vandoeuvre les Nancy-54506; France. E-mail : amar.rouane@lien.uhp-nancy.fr

This paper studies the microwave antenna characterization in intracardiac ablation for frequencies 915 and 2450 MHz. The theoretical study is validated by experimental measurements in vitro on electromagnetic phantom muscle tissue. The Specific Absorbed Rate (SAR) measurement setup is described. Two types of antennas have been designed, implemented and used, a monopoly antenna and a helical antenna. The Specific Absorbed Rate (SAR) and the measured reflection coefficient (S11) were obtained for antennas for the two frequencies. We show that each frequency can be adapted to a region where the ablation is necessary. According to the doctors, the goal is to have a lesion on the surface as the atria or in depth.

Key words*:* Cardiac ablation, microwave antenna, Specific Absorbed Rate, reflection coefficient

1. INTRODUCTION

FOR ARRHYTHMIA TREATMENT or conductive lesions, catheter intracardiac ablation is necessary for the destruction of morbid cells and it replaces the natural electric impulse by cardiac stimulator impulse.

The aim of this paper is to study the size of lesions that can occur with a catheter at different frequencies to see if these dimensions increase or decrease with frequency. To achieve this, a theoretical and a practical study are needed on the same model. This model must be the same for each frequency reflection coefficient (S11) and the same geometry as the antenna for the comparison criteria is justifiable.

Certain researchers have worked to improve the protocol [1], or design methods of temperature control [2] to prevent reaching tissue temperatures of 90 °C. Other teams have developed sources of energy like cryogenics [3, 4, 5, 6], ultrasound [7], Laser [8] and microwaves [9, 10, 11].

The goal of this research was to study lesion sizes obtained with a catheter at several frequencies in order to determine the most suitable frequency for cardiac ablation. A theoretical and a practical study were conducted on the same model using electromagnetic (EM) phantom muscle tissue. This model will have the same reflection coefficient (S11) and the same geometry for each frequency in order to have identical comparison criteria. During an EM ablation the lesion formation mechanism in cardiac tissue is based on conversion of the EM energy into calorific energy. Thus, in the theoretical approach the EM problem has to be solved.

The method used to solve this problem is based on the calculus developed by King [12]. This method uses a mathematical approximation allowing to obtain an analytic solution for Maxwell's equations in the near field inside a lossy medium.

2. METHOD

A. *Power deposition calculus*

To produce cardiac ablation we will be interested only in the near field where the temperature rise is maximal. The near field is determined by the value $\beta r \ll 1$ or $\beta = 2\pi/\lambda$ (λ wavelength in cardiac muscle).
We obtain:

- r<30mm at 2450 MHz
- r<70mm at 915 MHz

To solve this problem we will use the results developed by King [12] to determine the EM field generated by a monopoly in a lossy medium. The model used is shown in Fig.1.

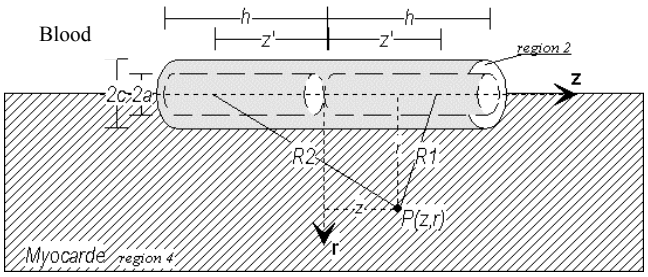

Fig.1. Dipole

This model is dipole with an inner conductor of radius ***a*** surround by a perfect dielectric (region2) of radius ***c*** inside an infinite medium (region 4). For point P(r,z) in region 4, we obtain the following equation for the electrical field along the z axis :

$$E_{4Z}(r,z) = \frac{i\omega\mu_0 I(0)}{4\pi \sin k_L h}\left[\left(1-\frac{k_L^2}{k_4^2}\right)\cdot\int_0^h \sin k_L(h-z')\left[\psi(z,z')+\psi(z,-z')\right]dz'\right.$$
$$\left.+\frac{k_L}{k_4^2}\left[\psi(z,h)+\psi(z,-h)-2\psi(z,0)\cos k_L h\right]+\frac{1}{2}\left(\frac{k_L^2}{k_2^2}-1\right)c^2\ln\frac{c}{a}\int_0^h \sin k_L(h-z')\right. \quad (1)$$

Where

$$\psi(z,z') = (e^{ik_4 R_1})/R_1 \qquad R_1 = \left[(z-z')^2+r^2\right]^{\frac{1}{2}}$$
$$\psi(z,-z') = (e^{ik_4 R_{21}})/R_2 \qquad R_2 = \left[(z+z')^2+r^2\right]^{\frac{1}{2}} \quad (2)$$

And

$$I(0) = V_0^e / Z_0$$
$$k_L = k_2\left[\frac{ln(c/a)+F}{ln(c/a)+n_{24}^2 F}\right]$$
$$F = \frac{H_0^{(1)}(k_4 c)}{k_4 c H_1^{(1)}(k_4 c)} \quad H: Function\ \ of\ \ Hankel \quad (3)$$
$$n_{24}^2 = k_2^2/k_4^2$$

The wave number k for each region is defined by:

$$k_2 = \omega(\mu_0\varepsilon_2)^{1/2}$$
$$k_4 = \omega\left[\mu_4\left(\varepsilon_4 + i\frac{\sigma_4}{\omega}\right)\right]^{1/2} \quad (4)$$

The values for ε_4 and σ_4 are calculated with the following formulas [13] in the frequency domain 0.01-18 GHz:

$$\varepsilon_4 = \varepsilon_0 \times \varepsilon_4' \quad (5)$$

Where

$$\varepsilon_4' = 1.71 f^{-1.13} + \frac{\varepsilon_s - 4}{1+(f/25)^2} + 4 \quad (6)$$

And

$$\sigma_4 = 1.35 f^{0.13}\sigma_0 + \frac{0.0222(\varepsilon_s - 4) f^2}{1+(f/25)^2} \quad (7)$$

σ_0 = 7 S/m, ε_S = 47 and f expressed in GHz. ε_S is the permittivity of blood.

We will check the following approximations:

$\left|k_4/k_2\right|^2 >> 1$ and $(k_2 c)^2 << 1$

With $\varepsilon_2 = \varepsilon_0 \times 2.1$, a = 0.24 mm and c = 0.8 mm, we obtain:

Frequencies	h (mm)	ε_4'	σ_4 (S/m)	$\left\|k4/k2\right\|^2$	$(k2c)^2$	$\left\|k4c\right\|^2$
2450 MHz	14.9	47	1.7	23.2	$3.5\ 10^{-3}$	$8.2\ 10^{-2}$
915 MHz	34.0	49	1.0	25.1	$4.9\ 10^{-4}$	$1.2\ 10^{-2}$
434 MHz	69.2	51	.86	29.8	$1.1\ 10^{-4}$	$3.3\ 10^{-3}$
27 MHz	876	148	.60	200	$4.3\ 10^{-7}$	$8.6\ 10^{-5}$

Table.1. Approximations of calculations based on the frequency.

Frequencies	k_2	k_4	k_L
2450 MHz	74	356+44i	108+23i
915 MHz	28	137+27i	47+8.2i
434 MHz	13	69+22i	23+3.6i
27 MHz	0.82	9.5+6.6i	1.8+0.16i

Table.2. Calculations of the wave number in the different medium as a function of frequency

The energy absorbed by the tissue is defined by:

$$SAR = \frac{1}{2}\sigma_4 E_{4Z}^2 \quad (8)$$

σ_4 is defined in (7) and calculated in Table 1.

The heat equation in tissue is solved using the finite difference method in order to obtain the temperature distribution around the antenna. This equation is obtained by combining heat transfer mechanisms in the heat equation.

$$\rho c \frac{\partial T}{\partial t} = \nabla(K \nabla T) - W_b C_b (T - T_a) + SAR \quad (9)$$

Where: SAR= Specific Absorption Rate J/m^{-3}
ρ Density kg. m^{-3}, c specific heat J.kg^{-1}.C^{-1}, K thermic conductivity W.m^{-1}.C^{-1}, W_b volumetric flux rate ml^3.kg^{-1}.C^{-1}, C_b blood specific heat J.kg^{-1}.C^{-1}, T_a ambient temperature °C.
The constants used are: Δr = 0.1 mm; Δt = 0.01 s; K = 0.7 W.m^{-1}.C^{-1}; ρ = 1000 kg.m^{-3}; c = 3930 J.kg^{-1}.C^{-1}; W_b = 200 ml^3.kg^{-1}.s^{-1}; C_b = 60 J.kg^{-1}.C^{-1}; T_a = 37 8C

3. Experimental setup

A. Method

Several researchers have proposed methods to measure the amplitude of electromagnetic field strength (EMF) and the SAR [14, 15].
SAR measurements were conducted using the setup presented in Fig.2. The EM probe was made by Narda model 8021B with the amplifier 8010B calibrated at 915 and 2450 MHz. A 2D map of the EM field was drawn along the z and r axis, each 0.25mm. Measurements were done with two different liquid phantoms for 915 and 2450 MHz. Their composition and electrical properties are presented in Table2.

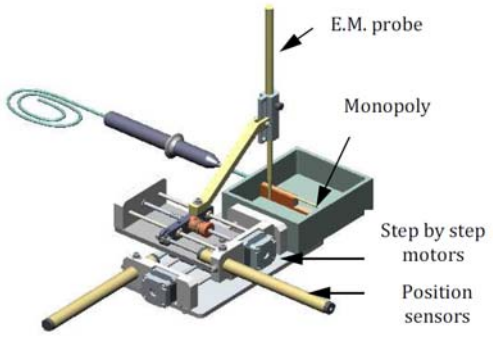

Fig.2. SAR measurement setup

The SAR measurement setup is composed of a probe mounted on 2 step motors connected to 2 positions sensors. This system is connected to an acquisition card controlled by a computer, which manages the control and record probe position and value of the EM field at each position (*HPVEE®software*) and performs the signal processing (*Mathematica®* s*oftware).*

B. Monopoly and helical antennas

The microwave generators used for this study are:
2450 MHz: generator 1000 from Fidus Medical Technology.
915 MHz: generator 15122 from MEL

These generators offer only an approximate value of the output power. Thus, two power sensors calibrated at 915 and 2450 MHz were used to give the real output power value. In order to study the lesion formation at 915 and 2450 MHz, two types of antennas were used: monopoly and helical antennas.

Monopoly at 915 and 2450 MHz have the following characteristics:

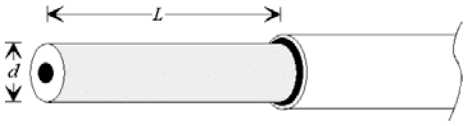

Fig.3. Monopoly

Frequency	d (mm)	L (mm)	S11 (dB)
915 MHz	1.225	31	-24
2450 MHz	1.225	12	-25

Table 2. Monopoly characteristics

These monopoly antennas were realized using the 50Ω coaxial cable IW70 from Insulated Wire Inc. The electrical and mechanical characteristics are:

- outer conductor outer diameter : 1.55mm
- inner conductor outer diameter : 0.48mm
- expanded Teflon dielectric :
  dielectric constant : ε'_r=1.44
  outer diameter: 1.22mm
- loss 1.24dB/m at 2450 MHz, 0.75 dB/m at 915 MHz

S11 measurements of these antennas were made using the network analyzer HP8752C. For each S11 measurement the antennas were immersed into liquid phantom having the same dielectric properties as cardiac tissue. At 915 MHz the phantom was made of 71% (in weight) ethylenglycol, 28% distilled water and 2% of NaCl [16]. At 2450 MHz the phantom was made of 67% (in weight) distilled water and 33% ethylenglycol [16]. The percentages of the composition permit to approach the values of pemittivities of the myocardium. The values of the permittivities of the myocardium depend on the frequency. Their dielectric properties are shown in Table4. These values were obtained by a network analyzer using the virtual line method [17].
Note that at high frequencies, the permittivity is defined by ε=ε'-jε" [15] where ε" represents the imaginary part and reflects the energy losses.

Frequenc	**Phantom composition**	**ε**	**ε''**
915 MHz	Ethylenglycol 71%, Water 28%, Salt 2%	5	25
2450	Water 67%, Glycérol 33%	6	17

Table 4. Dielectric properties of EM phantom

We work with antennas using two frequencies; thus we must prepare two phantoms for every given permittivity of the myocardium at the considered frequency.

Frequency	**ε'**	**ε''**
915 MHz	59	25
3450 MHz	57	14

Table 5. Dielectric properties of myocardium

S11 graph of the monopoly at 2450 MHz is presented in Fig.4. Both of these antennas show a good reflection coefficient: -24dB at 915 MHz
-25dB at 2450 MHz

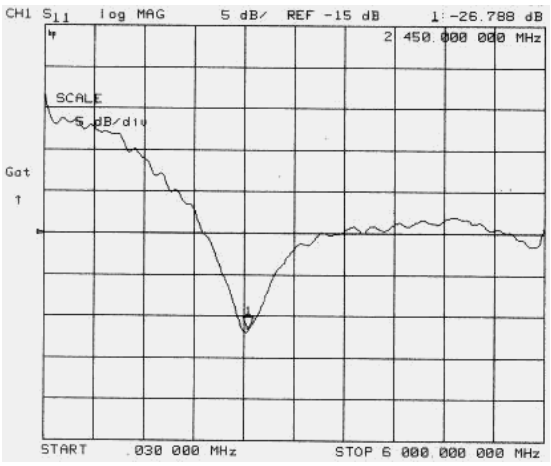

Fig.4. Monopoly S11 at 2450 MHz

Helical antennas used at 915 and 2450 MHz have the following characteristics:

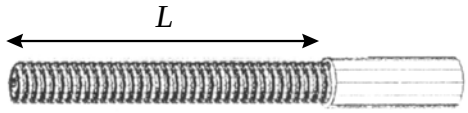

Fig.5. Helical antenna

Frequency	tours	L (mm)	S11 (dB)
915 MHz	52	26.2	-17
2450 MHz	49	24.7	-17

Table 6. Helical antenna characteristics

Two types of coaxial cables were used to realize these antennas: IW70 at the beginning of the catheter and IW50 near the antenna. The IW50 cable is used because of its smaller diameter that allows proper bending of the catheter. The characteristics of this coaxial cable are:

- outer conductor outer diameter : 1.1mm
- inner conductor outer diameter : 0.32mm
- expanded Teflon dielectric : dielectric constant : ε'_r=1.37
  outer diameter : 0.80mm
- loss 1.83dB/m at 2450 MHz, 1.14 dB/m at 915 MHz

S11 graph of the 2450 MHz helical antenna is presented in Fig.6. SAR measurements of these antennas gave the following results. For the monopoly shown in Fig.7, the 2D SAR plots at 915 MHz and 2450 MHz are shown in Fig.8 and 9, where iso-SAR lines were drawn at 5, 10 and 20%.

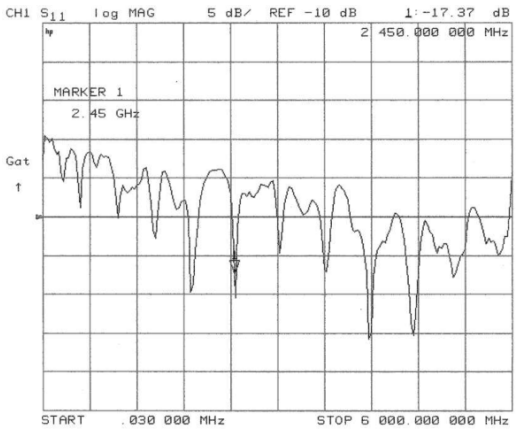

Fig.6. Helical antenna S11

This graph shows that the antenna exhibits several adaptation frequencies. Thus, it is easy to adapt this antenna at 915 MHz without significantly changing the length of the antenna. It is not the case for the monopoly antenna which presents only one frequency adaptation. However, we should keep in mind that this does not mean that the energy distribution around the antenna will be homogenous; it only means that the transfer of energy between the coaxial cable and the antenna is optimal.

4. RESULTS

We can see a strong SAR peak around z = 0mm on these figures. These results correspond to the calculus obtained by King that shows a maximum of the electrical field at the beginning of the antenna.

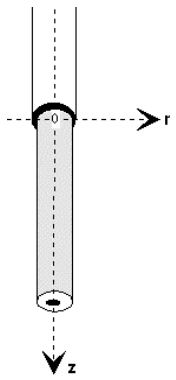

Fig.7. Monopoly antenna axis

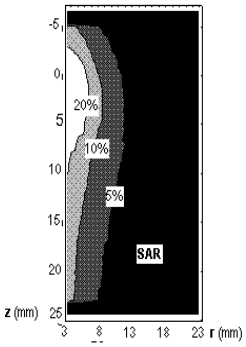

Fig.8. 915 MHz Monopoly antenna SAR

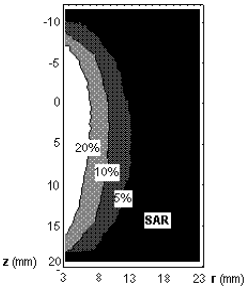

Fig.9. 2450 MHz Monopoly antenna SAR

Results obtained with the helical antenna, Fig.10, are shown in Fig.11 and 12:

Fig.10. Helical antenna axis

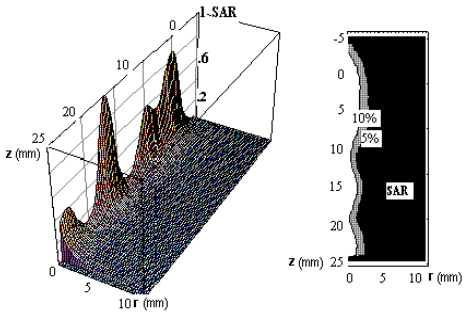

(a) *(b)*

Fig.11. 915 MHz Helical antenna SAR.

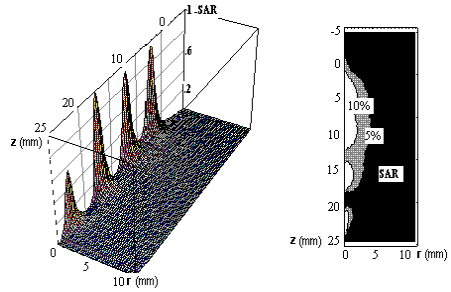

(a) (b)

Fig.12. 2450 MHz Helical antenna SAR

As we can see on these curves, the SAR pattern is more homogenous but does not penetrate deep into the helical antenna case as compared to the monopoly antenna.

5. DISCUSSION

The figures obtained from the SAR measurements show similar results to those obtained from monopoly probes in [18, 19], and those obtained for the helical antennas in [20]. We can better appreciate the results in Fig.11b and 12b. They show that there is no difference regarding the depth of penetration between 915 and 2450 MHz; the theoretical calculation gives the same results. There are, however, notable differences in SAR profiles if we consider the longitudinal axis of the antenna (z-axis). For monopoly probes, there is a peak SAR at the beginning of the antenna where z = 0 and a decrease of it as z increases. The general shape of the SAR is due to radiation losses throughout the antenna, which are obviously lower at the beginning of the antenna and very strong at the end of it. The lengths of antennas at 915 MHz and 2450 MHz are not the same; the profile of SAR is more extended to 915 MHz. Nevertheless, at 2450 MHz, the profile of the SAR is more homogeneous which in case of cardiac ablation is very important. Indeed, this avoids having hot spots in the region very close to the antenna that can cause the formation of blood clots and in that case create a risk of embolism. For the antennas of helical type the case is different because antennas are the same length and we have a structure which slows down the phase**.** As we can see, all along the antenna there are very important SAR spikes, very close together. This is quite typical for this type of structure.

This ensures a good homogenization of the profile of SAR, but as we can see, the depth of penetration of this type of antenna is quite small compared to the monopoly antenna. Indeed, it has a very important surface wave and this can cause problems if one tries to create deep lesions without charring the surface.

Nevertheless, this type of lesion may be suitable to the atria where we rather need a lesion on the surface than in depth.

6. CONCLUSION

The comparative study of intracardiac ablation between frequencies 915 and 2450 MHz has been conducted from a theoretical and practical point of view. The results show an

agreement between the theoretical and experimental study, which allowed us to validate the theoretical study. This study shows that there are no significant differences compared to the depth of penetration between the different frequencies. The proper choice for cardiac ablation, between the different frequencies studied, won't be in terms of depth of penetration, but rather on the geometry of lesions to be created.

Another criterion for the choice of frequency also concerns technological possibilities associated with each frequency, and the manufacturing cost. This applies to the generator and the catheter. For example, the generator will be easier to design at 915 MHz because the development of mobile devices with frequencies around 1 GHz has allowed the marketing of many integrated circuits operating at 1 GHz. The catheter losses in the cable will be less important at low frequencies, so it will be possible to use small diameter cables because the wavelength and the risk of coupling with the thread of ECG can be problematic. The compromise to be adopted will be dictated by the wishes and objectives of doctors and also subject to technological limitations of each frequency.

7. REFERENCES

[1] Nakagawa H, Yamanashi WS, Pitha JV, Comparison of in vivo temperature profile and lesion geometry for radiofrequency ablation with a saline-irrigated electrode versus temperature control in a canine thigh muscle preparation. *Circulation*; 91:2264-2273, 1995.

[2] Jaïs P, Haïssaguerre M, Shah DC et al : Successful irrigated-tip catheter ablation of atrial flutter resistant to conventional radiofrequency ablation. *Circulation*; 98: 835-838, 1998.

[3] Dubuc M, Skanes A, Roy D, Thibault B, Talajic M, Guerra P : Catheter cryomapping and cryoablation of supraventricular rachycardia in man : preliminary results (abstract) . *PACE*; 23 (II): 613, 2000.

[4] P. Khairy and al.; Enlargement of catheter ablation lesions in infant hearts with cryothermal versus radiofrequency energy: An animal study; circ. Arrhythm. Electrophysiol; 4; 211-217; 2011

[5] J. Philip Saul; D'ont forget to gather the evidence: myocardial effects of cryoablation in the immature heart. Circ. Arryhthm. Electrophysiol.; 4; 123-124; 2011.

[6] Z. Gao and al; Direct measurement of the lethal isotherm for radiofrequency tissue. Circ. Arryhthm. Electrophysiol.; 4; 373-378; 2011.

[7] M.D. Lesh, J. Diedrich, P.G. Guerra, Y. Goseki, P.B. Sparks : An anatomic approach to prevention of atrial fibrillation : Pulmonary vein isolation with through-the-balloon Ultrasound ablation. Thorac. Cardiovasc. Surg., 47 (Suppl.): 347-351, 1999.

[8] R. Svenson, L. Littman, R. Splinlen : Application of lasers for arrhythmia ablation. In Zipes D.; Jalife J. (eds) : Cardiac Electrophysiology from cell to Beside. Philadelphia, WB Saunders, 989-997, 1990.

[9] S.G. Splitzer, P. Richter, M. Knaut, S. Schuler: Treatment of atrial fibrillation in open heart surgery. The potential role of microwave energy. Thorac. Cardiovasc. Surg., 47 (Suppl.), 374-378, 1999.

[10] P. Adragao, L. Parreira, F. Morgado, D. Bonhorst, R. Seabra-Gomes : Microwave ablation of atrial flutter. PACE, 22:1692-1695, 1999.

[11] B.A. Vanderbrink, C. Gilbride : Safety and efficacy of a steerable temperature monitoring microwave catheter system for ventricular myocardial ablation, J. Cardio. Electrophysiology, 11:305-310, 2000.

[12] R.W.P. King, B.S. Trembly, J.W. Strohbehn : The electromagnetic field of an insulated antenna in a conducting medium. IEEE Trans. Microwave Theory Tech., vol. 31, pp. 574-583, 1983.

[13] Polk C., Postow E. : CRC Handbook of Biological Effect of Electromagnetic Fields. CRC Press, 1986.

[14] J. Klima, R. Ščehovič: The field strength measurement and SAR experience related to human exposure in 110MHz to 40 GHz; Measurement Science review, Vol.6; Section2, N°4, pp.40-44, 2006.

[15] K. Watanabe, Y. Taka, O. Fujiwara: Cole-Cole measurement of dispersion properties for quality evaluation of red wine; Measurement Science Review, Vol. 9, N°5, pp.113-116, 2009.

[16] C.K. Chou, G.W. Chen, A.W. Guy, K.H. Luk : Formulas for preparing phantom muscle tissue at various radiofrequencies. Bioelectromagnetics, vol.5, pp. 435-441, 1984.

[17] D. Bérubé, F. M. Ghannouchi, P. Savard, I. Jolicoeur : A Comparative study of four open-ended coaxial probe models for permittivity measurements of lossy dielectric/biological material at microwave frequencies. IEEE Trans. M.T.T., vol. 44 (part II), pp. 1928-1934, 1996.

[18] Labonte, A. Blais, R. Legault, H.O. Ali, L. Roy : Monopole Antennas for microwave catheter ablation. IEEE Trans. Microwave Theorie Techn., vol.44, pp. 1848-1854, 1996.

[19] J.C. Camart, J.J. Fabre, B. Provost, J. Pribetich, M. Chive: Coaxial antenna array for 915 MHz interstitial hyperthermia : Design and modelization - Power deposition and heating pattern - Phased array. IEEE Trans. Microwave Theory Tech., vol.40, pp. 2243-2250, 1992.

[20] M.S. Mirotznik, N. Engheta, K.R. Foster: Heating characteristics of thin helical antennas with conducting cores in a lossy medium - I : Noninsulated Antennas. IEEE Trans. Microwave Theory Tech., vol.41, pp. 1878-1886, 1993.

Received November 8, 2011.
Accepted February 28, 2012.